

Numerical Study on the Mechanical Behaviour of Hollow-box Beams Subjected to Static Loading

Hugo M. SILVA
José Filipe MEIRELES
*Department of Mechanical Engineering
University of Minho
Campus of Azurém
4800-058 Guimarães, Portugal
hugolopessilva@gmail.com
meireles@dem.uminho.pt*

Received (11 June 2017)
Revised (21 November 2017)
Accepted (8 December 2017)

Novel types of internally reinforced thin-walled beams are subjected to a feasibility analysis in terms of their effective mechanical behaviour. The novel beams are subjected to bending and torsion uncoupled loadings and are analysed in terms of their stiffness behaviour in static analysis. The models were built using the commercial Finite Element Method (FEM) software ANSYS Mechanical APDL. The feasibility of the models was determined by the comparison of the stiffness behaviour of the novel beams with simple hollow-box beams, having the same mass and dimensions, with the exception of the thickness. An efficiency parameter is used in order to determine the feasibility of the studied geometries. It is found that the novel geometries represent a great improvement under bending loading, better than under torsion loading. Nevertheless, for bending and torsion combined loadings, if bending loads are predominant, the beams can still be interesting for some applications, in particular those with mobile parts.

Keywords: sandwich beams, mechanical behaviour, FEM – Finite Element Method, solid mechanics.

1. Introduction

The acceleration of industrial machines mobile parts has been increasing over the last few years, due to the need of higher production in a short period of time. The machines were dimensioned for a lower value of acceleration, which means there is not enough stiffness for the correct operation at much higher accelerations. There is the need of improving stiffness to make possible the correct machine operation without undesired vibrations that can ultimately lead to failure [1]. There is also the need of using low-weight and stiff structures in engineering applications involving

mobile parts, such as laser cutting machines and plotters [1,2]. This need balancing of structural solutions which are suitable for these requirements, such as the sandwich geometries. It is found that to improve stiffness, changing the geometry has a higher effect than materials selection [2]. This work is about the study of thin-walled beams which are made entirely of steel. All-metal sandwich structures have high weight efficiency [3–5], multifunctional characteristics, and are highly resistant to impact [4, 6–9]. The objective of using sandwich panels is the possibility of reducing weight while preserving the stiffness. The transportation industry is where the use of sandwich panels leads to economical savings, because, due to the possibility of weight reduction, the fuel consumption may decrease [10]. Silva and Meireles studied various sandwich geometries in order to evaluate its effective mechanical behaviour [11,12]. They also studied the feasibility of incorporating sandwich panels in reinforced hollow-box beams for industrial applications. The authors presented similar structures to the ones of this work, however, without transversal reinforcements [13]. The application of the present work is industrial laser cutting machines, but can also be used in plotters. A vast number of initial solutions were evaluated, and an adaptation was done in order to incorporate the best ones into the novel hollow-box beams. The novel types of sandwich beams under bending and torsion uncoupled loadings built in ANSYS show good results under bending loading, better than under torsion loads. However, further presented results for the Beam 1, Pattern 4 represents an improvement both under bending and torsion loadings.

2. Numerical procedure

2.1. The FEM models

Finite Element Method (FEM) models were built in the commercial FEM program ANSYS Mechanical APDL. Those models represent the novel beams. They are composed of two sandwich panels on the top and on the bottom, and a reinforcement pattern on the sides, as shown in Fig. 1.

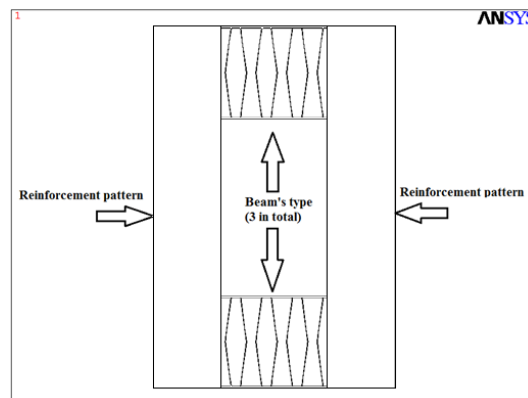


Figure 1 Configuration of beam types (cf. Figure 6)

Simple hollow-box beams, named hollow-solid sections (HSS), and abbreviated as HSS in the results were also studied, using the same conditions as on the sandwich beams. Figure 2 shows the areas of the FEM of the HSS beam.

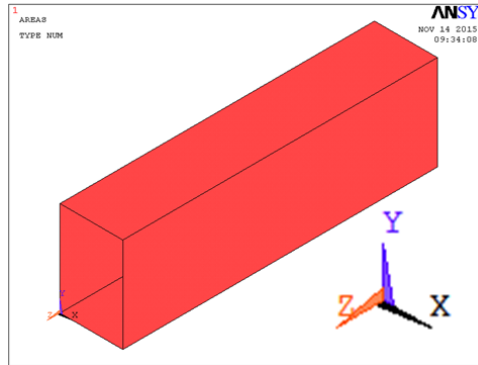


Figure 2 Areas of the FEM model representing the HSS of simple beam

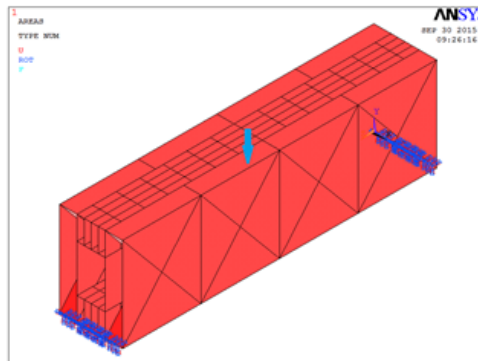


Figure 3 DOF constraints and loading in bending

The used element was SHELL63 (Shell Elastic 4 nodes). The elements are of the free quadrilateral type with a mean length of 0.0025 m. The mesh is fine enough to obtain converged results. The beam was constrained in the lines of the extremities ($z = 0$ and $z = 1$, along the beam), the support type simply supported at its ends, as shown in the Fig. 3.

Concentrated loads were used by simplification in order to simulate the action of bending and torsion. Bending was applied by one concentrated load of 1500 N, on the centre of the top face, as shown in Fig. 3. Torsion is applied by means of a binary load of 2000 N (Fig. 4).

The results were measured on the points P_1 and P_2 (Fig. 5), and the average between the two was calculated in every case. The global maximum is less relevant than local values due to the fact that in the practical application, the loads may be more distributed than in this case. The maximum absolute values could be taken instead, but the comparison would be erroneous because the novel beams are of much lower thickness and the effect of the concentrated load is amplified than it would be in the respective HSS beams.

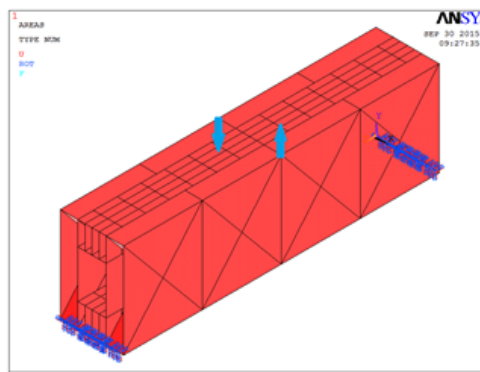


Figure 4 DOF constraints and loading in torsion

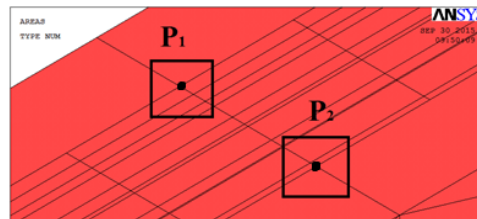


Figure 5 Measuring points P_1 and P_2 under bending load

The same measuring points as in bending were also used in case of torsion loading. In Figs. 6–9 the applied geometries of the novel beams are presented.

Figure 10 shows the internal reinforcement of the beam B3, Pattern 3. The top area was unselected to allow inner view. The transversal reinforcements along the length of the sandwich geometry are also present at the bottom panel and are common to all the beams (B1, B2 and B3).

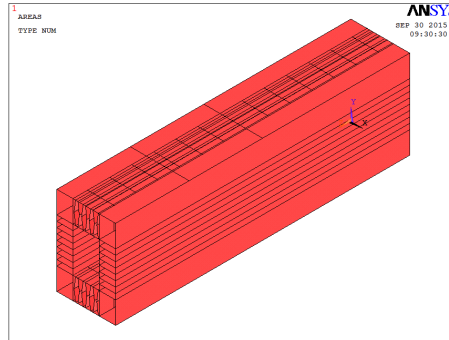


Figure 6 Geometry of one of the novel beams illustrating Pattern 1. Here, Beam 3 is shown without its transversal ribs

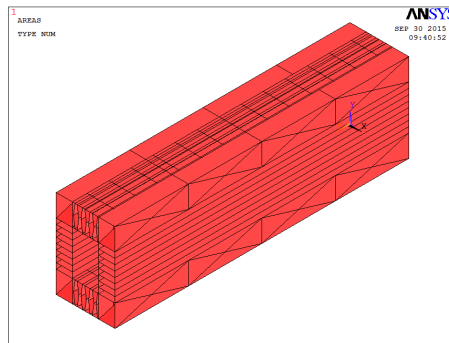


Figure 7 Geometry of one of the novel beams illustrating Pattern 2. In this case, Beam 3 is presented without its transversal ribs

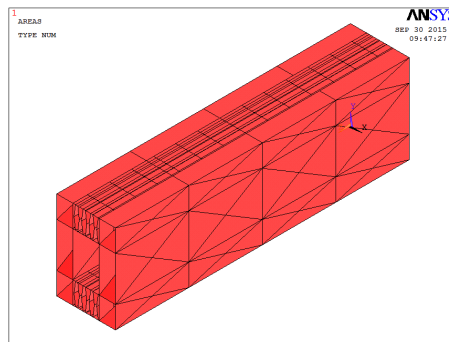


Figure 8 Geometry illustrating Pattern 3. In this case, the shown beam is Beam 3 without transversal ribs

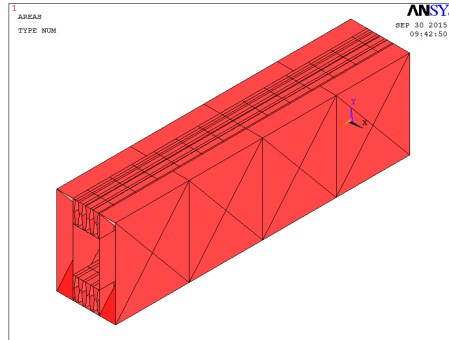


Figure 9 Geometry of one of the novel beams illustrating Pattern 4. The presented beam is Beam 3 without transversal ribs

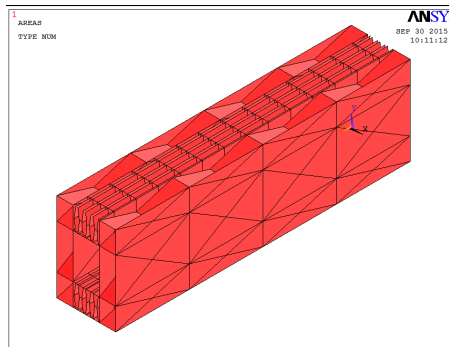


Figure 10 Internal reinforcements on Beam 3, Pattern 3

Assumed geometry of the flanges is shown in Fig. 11.

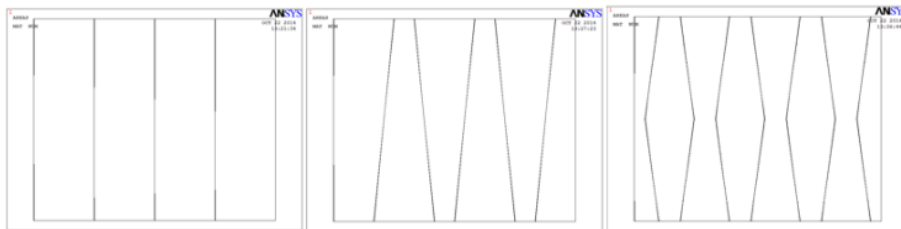


Figure 11 Section view of the sandwich beams: web-core (left, Beam 1), corrugated-core (middle, Beam 2) and honeycomb core (right, Beam 3)

The material used is steel, with the properties shown in Tab. 1 of the Chapter 3. The simple beams have their thickness adjusted in order for the mass to match the novel beam one being compared with. The thickness is 0.002 m for every novel

beam. Table 1 summarizes mass and thickness values taken to calculation of each simple beam model.

Table 1 Models mass and thickness values assumed in calculations of simple beams

	A1	A1 HSS	A2	A2 HSS	A3	A3 HSS
	m [kg]	t [m]	m [kg]	t [m]	m [kg]	t [m]
Pattern 1	50.7	0.0064	55.6	0.0070	60.4	0.0077
Pattern 2	58.8	0.0075	63.6	0.0081	68.5	0.0087
Pattern 3	51.4	0.0065	56.3	0.0071	61.1	0.0077
Pattern 4	42.2	0.0053	46.9	0.0059	51.8	0.0066
	B1	B1 HSS	B2	B2 HSS	B3	B3 HSS
	m [kg]	t [m]	m [kg]	t [m]	m [kg]	t [m]
Pattern 1	53.6	0.00679	58.3	0.00739	63.2	0.00801
Pattern 2	61.6	0.00781	66.4	0.00841	71.2	0.00903
Pattern 3	53.0	0.00688	59.1	0.00748	63.9	0.00810
Pattern 4	49.0	0.00570	49.7	0.00630	56.0	0.00691

2.2. Feasibility criterion

The feasibility of the novel beams developed in this work is evaluated under bending and torsion uncoupled loadings. An improvement factor is defined to determine the feasibility. Under bending loads, the improvement can be calculated as:

$$\text{Imp}_{\delta_b}(\%) = \frac{|\delta y_{HSS}| - |\delta y_{nb}|}{|\delta y_{nb}|} \cdot 100\%, \quad (1)$$

where:

δy_{nb} is the average deflection [m] of the novel beam measured at points P_1 and P_2 , (Fig. 5),

δy_{HSS} is the average deflection [m] of the simple hollow-box beam measured at the same points (Fig. 5),

Imp_{δ_b} is the feasibility of the novel beam in comparison with the simple hollow-box beam under bending loading.

Under torsion loading, the results were also measured on the points P_1 and P_2 (Fig. 5), and the improvement in terms of twist angle is given by eq. (2):

$$\text{Imp}_{\theta_t}(\%) = \frac{|\theta_{HSS}| - |\theta_{nb}|}{|\theta_{nb}|} 100\% \quad (2)$$

where:

θ_{nb} is the average angular deflection of the novel beam measured at points P_1 and P_2 , [rad],

θ_{HSS} is the average angular deflection of the simple hollow-box beam measured at the same points [rad],

Imp_{θ_t} is the feasibility of the novel beam in comparison with the simple hollow-box beam under torsion loading in terms of twist angle.

The feasibility in terms of the y deflection under torsion loading was calculated by:

$$Imp_{\delta_t}(\%) = \frac{|\delta y_{HSS}| - |\delta y_{nb}|}{|\delta y_{nb}|} 100\%. \quad (3)$$

where:

δy_{nb} is the average deflection of the novel beam measured at points P_1 and P_2 [m], (Fig. 5). The absolute value of the deflections is considered for the calculation of the average deflection, both in the case of the simple beam and the novel beams,

δy_{HSS} is the average deflection of the simple hollow-box beam measured on the two points [m], (Fig. 5),

Imp_{δ_t} is the feasibility of the novel beam in comparison with the simple hollow-box beam under torsion loading.

3. Results

3.1. Mesh sensitivity analysis

In order to ensure the accuracy of the Finite Element results, a mesh sensitivity analysis was performed, both under bending and torsion loadings. The deflection results were taken from the point P_1 and P_2 of the Pattern 3 of each beam (three in total). The models of the Pattern 3 were chosen due to the fact that they are the most complex of all four patterns. As such, if the mesh is fine enough to obtain converged results for the Pattern 3, it is expected that the mesh is also fine enough for all the other models of the other patterns. The mesh was refined from a length of 0.02 m to 0.0025 m in three refinement levels, as in the Sec. 3 (Tab. 3.5). In each stage, the mean element size turned into half of the previous. It was arbitrated that the mesh is fine enough for a specific model if the error is lower than 0.5%. A lower value could be considered, but further mesh refinement implies a much longer solution processing time, which was already between 20 and 40 minutes per model on a machine with Core i5 at 2.5 Ghz processor equipped with 16 GB of RAM. Further refinements would imply many days or even weeks in obtaining optimum solutions in optimization processes (Sec. 5), without a great improvement in the accuracy of the results.

3.1.1. Bending

Figures 12 and 13 show the mesh sensitivity results for bending load at points P_1 and P_2 , respectively.

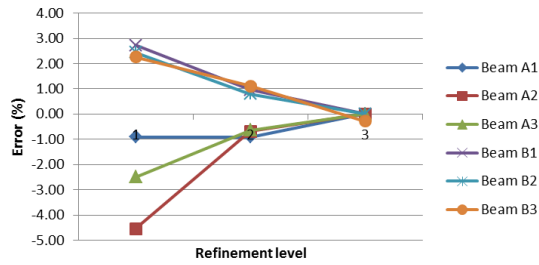


Figure 12 Mesh sensitivity results for the point P_1 under bending load for Pattern 3

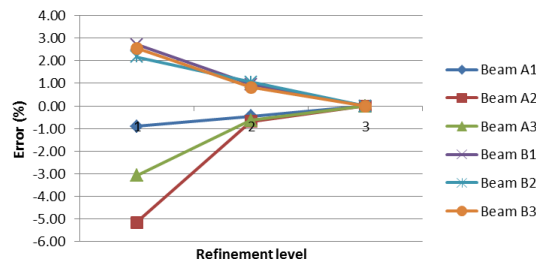


Figure 13 Mesh sensitivity results for the point P_2 under bending load for Pattern 3

3.1.2. Torsion

Figures 14 and 15 show the mesh sensitivity results for torsion load at points P_1 and P_2 , respectively.

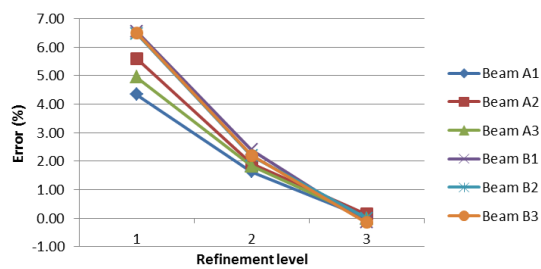


Figure 14 Mesh sensitivity results at the point P_1 under torsion load for Pattern 3

These results allow to conclude, that, for every case, a refinement level 3, representing a mesh size of 0.0025 m is needed to obtain results with error lower than 0.5%.

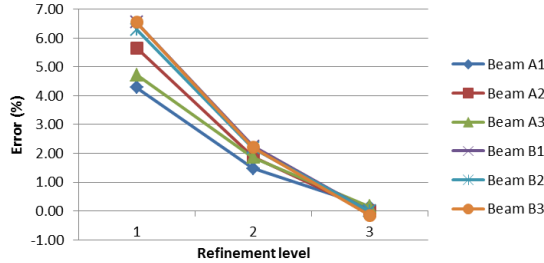


Figure 15 Mesh sensitivity results at the point P_2 under torsion load for Pattern 3

3.1.3. Feasibility results

The FEM simulations were performed in the elastic domain. The results were measured on the points P_1 and P_2 . The results of all models are compared with conventional beams having the same weight, and modelled using the same conditions. The deflection of the beams (Figs. 16–21) was determined using eqs. (1–3) as improvement (Imp) of a novel beam in relation to its conventional version.

3.2.2.1 Bending

Figure 16 presents deflections and improvement in results regarding hollow solid sections (HSS) and novel beams under bending loading. Figure 17 presents improvement in deflections under bending loading, using formula (1). These results allow discussion of feasibility of novel beams comprising sandwich beams under uncoupled bending and torsion loadings. All the obtained deflections δ of the novel beams are lower than for every HSS beam under bending load. The maximum improvement is close to 4100%, and happens for the beam A1, pattern 4.

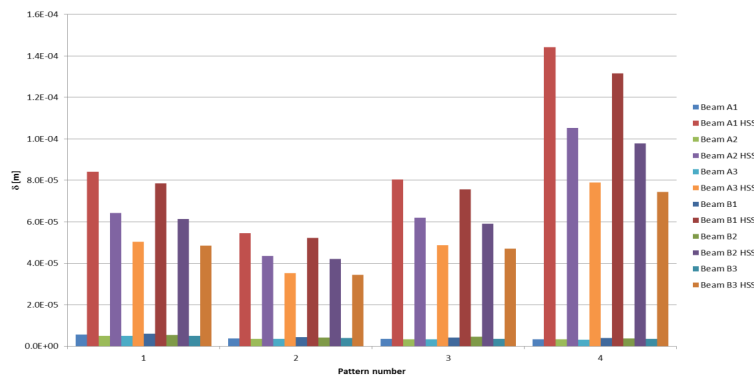


Figure 16 Deflection of all beams under bending load

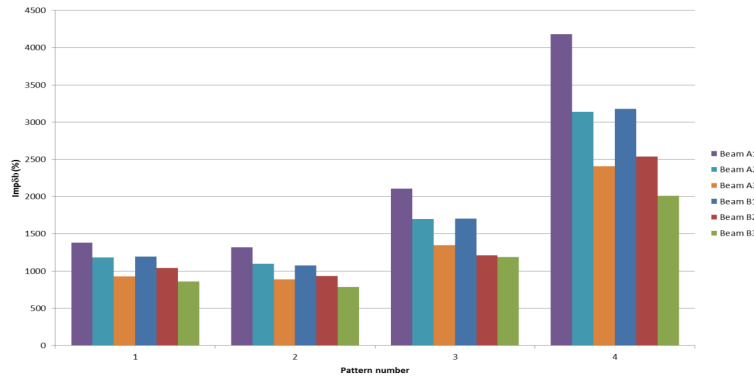


Figure 17 Boundary conditions applied to the FEM model

3.2.2.2 Torsion

In Fig. 18 angular deflection regarding hollow solid sections (HSS) and novel beams under torsion loading respectively, is presented.

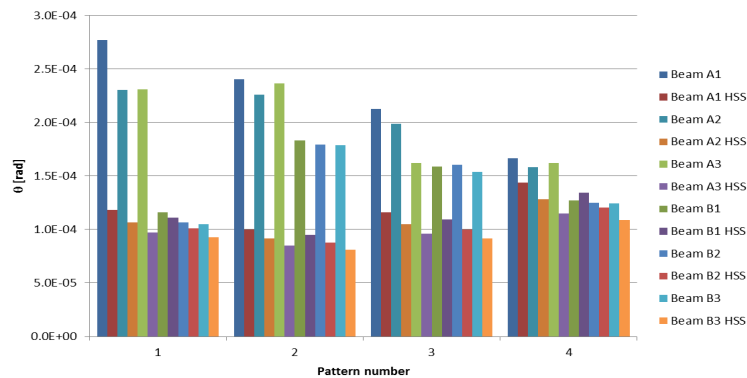


Figure 18 Rotation angle of all studied beams under torsion load

Figure 19 shows the improvement in angular deflections under torsion loadings, calculated using formula (2). Under torsion loading, there appears a worsening in the θ , except for the beam B1, pattern 4. When analysing deflections in torsion, the Pattern 1 of all three beams also show good results, but this behaviour may happen because the transversal reinforcement that exists at the midspan is quite effective in reducing deflections. In Fig. 20 deflections regarding hollow solid sections (HSS) and novel beams under torsion loading, respectively are shown.

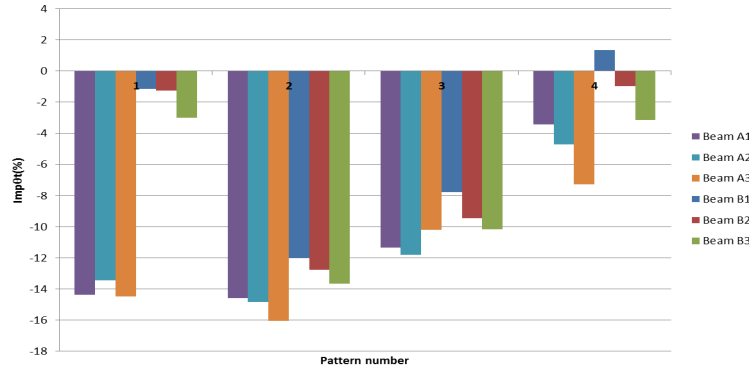


Figure 19 Improvement of all studied beams under torsion load

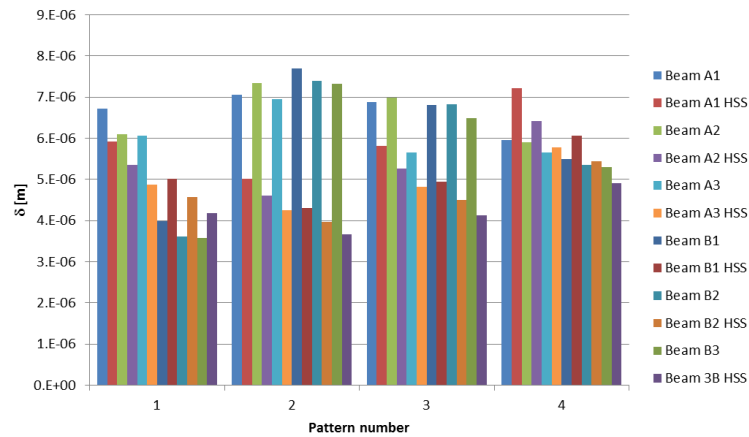


Figure 20 Deflection of all beams under torsion load

Improvement in deflections under torsion loading calculated with formula (3) is presented in Fig. 21. As a conclusion can be stated that models B1, B2 and B3 utilizing Pattern 1 and models A1, A2, A3, and B1 of pattern 4 originate an improvement under torsion loadings. These models represent an improvement both under bending and torsion loadings.

4. Discussion of results

It is shown that under bending loading, the improvement of the sandwich beam in relation to the conventional beam is between 1400% and 4200% for the beam A1, 1200% and 3100% for the beam A2, and 900% and 2400% for the beam A3, approximately. For the beams with transversal reinforcements, the improvement of the sandwich beam in relation to the conventional beam is between 1200% and 3100% for the beam B1, 1000% and 2500 % for the beam B2, and 800% and 2000%

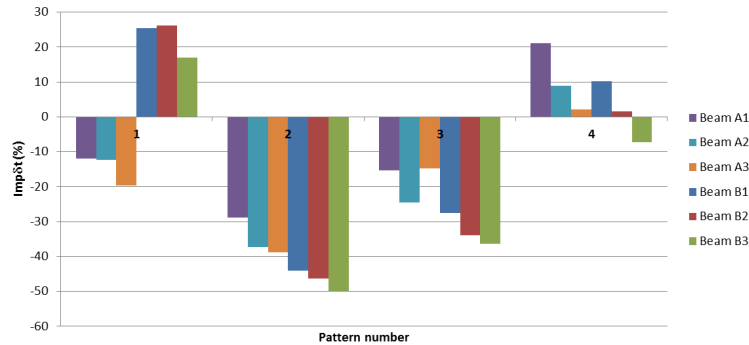


Figure 21 Improvement under torsion load

for beam B3, approximately. It is possible to see that, in spite of the lower number of longitudinal ribs at the flanges, the beam A1 is still the most effective of all geometries.

Under torsion loadings, the improvement results regarding y -axis deflection for beams without transversal reinforcements range from approximately -30 to $+20\%$ for the beam A1, -40 to $+10\%$ for the beam A2, and -40 to $+2\%$ for the beam A3. For beams with transversal reinforcements, δ varies from -40 to $+25\%$ for the beam B1, -45 to $+26\%$ for the beam B2, and -50 to $+18\%$ for the beam B3, approximately.

Twist angle θ improvement values vary between -14% and -4% for the beam A1, -15% to -3% for the beam A2 and -16% to -7% for the beam A3. The improvement of θ varies between -12% and $+1\%$ approximately for the beam B1, -13% and -1% for the beam B2, and from -14% to -3% for the beam B3. Negative values of improvement represent a worsening of the stiffness behaviour in relation to conventional hollow-box beams.

5. Conclusions

It is possible to conclude that, both under bending and torsion loadings, the Beam 1 with Pattern 4 presents the best results. It is possible to conclude that, in spite of the general worsening under torsion loads, the improvement under bending loads can overcome the worsening, especially for the models Beam 1, pattern 4. The beams developed can be of interest for applications where light and stiff structures must be used, such as in laser cutting machines and plotters. This paper presented a novel type of beams and aimed to assess its feasibility for industrial applications. It can be concluded that the novel beams represent a great improvement over HSS beams under bending loadings, much more than under torsion loadings. The next task is to optimize the mechanical behaviour, most importantly under torsion load, but also under bending one. Under bending loading, the sandwich panels are effective in withstanding deflections due to the high value of the moment of resistance originated by the height of the sandwich component. The reinforcements on the sides of the beam were designed for torsion: the transversal plates are very effective in increasing the torsional inertia moment of the system, which determines the stiffness behaviour

under torsion. Diagonal ribs are shown to be effective under torsional loadings, so they were also added to the sides of the models [14].

References

- [1] **Silva, H.M., De Meireles, J.F.:** Determination of material/geometry of the section most adequate for a static loaded beam subjected to a combination of bending and torsion, *Materials Science Forum*, 730-732, 507–512, **2013**.
- [2] **Silva, H.M.:** Determination of material/geometry of the section most adequate for a static loaded beam subjected to a combination of bending and torsion, MSc. Thesis, University of Minho, **2011**.
- [3] **Ashby, M.F., Evans, A.G., Fleck, N.A., Gibson, L.J., Hutchinson, J.W. and Wadley, H.N.G.:** *Metal foams: A design guide*, Butterworth Heinemann, Boston, **2000**.
- [4] **Evans, A.G., Hutchinson, J.W., Fleck, N.A., Ashby, M.F. and Wadley, H.N.G.:** The topological design of multifunctional cellular metals, *Progress in Materials Science*, 46, 309–327, **2001**.
- [5] **Wadley, H.N.G, Fleck, N.A., Evans, A.G.:** Fabrication and structural performance of periodic cellular metal sandwich structures, *Composites Science and Technology*, 6316, 2331–2343, **2003**.
- [6] **Hutchinson, R.G., Wicks, N., Evans, A.G., Fleck, N.A. and Hutchinson, J.W.:** Kargone plate structures for actuation, *International Journal of Solids and Structures*, 4025, 6969–6980, **2003**.
- [7] **Qiu, X., Deshpande, V.S. and Fleck, N.A.:** Finite element analysis of the dynamic response of clamped sandwich beams subject to shock loading, *European Journal of Mechanics A- Solids*, 226, 801–881, **2003**.
- [8] **Xue, Z.T, Hutchinson, J.W.:** Preliminary assessment of sandwich plated subject to blast loads, *International Journal of mechanical sciences*, 454, 687–705, **2003**.
- [9] **Fleck, N.A., Deshpande, V.S.:** The resistance of clamped sandwich beams to shock loading, *Journal of Applied Mechanics*, 713, 386–401, **2004**.
- [10] **Léotoing, L., Drapier, S. and Vautrin, A.:** Nonlinear interaction of geometrical and material properties in sandwich beam instabilities, *International Journal of Solids and Structures* 39, 717–3739, **2002**.
- [11] **Silva, H.M., De Meireles, J. F.:** Effective Mechanical Behavior of Sandwich Beams under Uncoupled Bending and Torsion Loadings, *Applied Mechanics and Materials*, 590, 58–62, **2014**.
- [12] **Silva, H.M., De Meireles, J. F.:** Effective Stiffness Behavior of Sandwich Beams under Uncoupled Bending and Torsion Loadings, 852, 469–475, **2016**.
- [13] **Silva, H.M., De Meireles, J.F.:** Feasibility of Internally Reinforced Thin-Walled Beams for Industrial Applications, *Applied Mechanics and Materials*, 775, 119–124, **2015**.
- [14] **Weckman, R.:** Diagonal ribs increase torsional rigidity, **1988**.